

Velocity Profiles in Perforated Completions

J.H. ENG, D.B. BENNION, J.B. STRONG

Hycal Energy Research Laboratories Ltd.

Abstract

The productivity of perforated completions is greatly reduced when fines are mobilized causing particles to plug pore throats within a formation. Even in clean sands, relatively large quantities of particulate matter are present. Mobilization of these fines occurs as fluid velocities exceed critical levels which may be determined experimentally in tests performed on core samples. The results of these tests, however, provide linear velocities which must be correlated to account for irregular flow patterns in the near wellbore region.

A three-dimensional simulator is developed to analyze the velocity profiles in the vicinity of a perforation. By assuming a simplified geometry in which multiple perforations are carried out at uniform vertical intervals in a radially symmetric manner, maximum velocities in the region surrounding a perforation are quantified. Thus, for a given injection or production rate, actual velocities can be calculated allowing direct correlation of laboratory displacement test results.

Introduction

The migration of small solid materials ("fines") within porous media has long been recognized as a source of potentially severe permeability impairment in formations containing oil and gas. Fines migration occurs when loosely attached particles are mobilized by fluid drag forces caused by the motion of fluid within the pore space. If a sufficient quantity of large enough fines are mobilized, they can collect at pore throats within the medium and cause permeability impairment. Muecke⁽¹⁾ documents how a variety of different types of fines such as clay minerals, quartz, amorphous silica, feldspars, mica and carbonates can be susceptible to migration. Gray and Rex⁽²⁾ reported the migration of mica needles and kaolinite. They also found that migration could be induced by salinity changes or abrupt reductions in the ratio of divalent to monovalent ions present in the brines. Morgan⁽³⁾ investigated changes in pH and salinity with respect to fines migration.

Muecke⁽¹⁾ documented how fines mobilization generally occurs only when the phase which wets the fines is in motion. For example, there are many cases of severe fines mobilization occurring in water-wet reservoirs during waterfloods only after the water breaks through to the producing wells.

Other authors including Porter⁽⁴⁾, Selby⁽⁵⁾, Kwan⁽⁶⁾, Prisholm⁽⁷⁾, Gabriel⁽⁸⁾, Borchardt⁽⁹⁾, and Sengupta⁽¹⁰⁾ have documented phenomena which affect fines migration. Gruesbeck and Collins⁽¹¹⁾ describe a detailed phenomenological theory of entrainment and deposition of fines in porous media.

Laboratory Tests to Evaluate Fines Mobilization

An important parameter to be determined in the laboratory is the critical interstitial velocity (actual velocity in the pore space) at which fines mobilization begins to occur.

The tests are commonly conducted on short cylindrical core samples (generally 2.54 to 3.81 cm in diameter by 4 to 8 cm in length). The samples are generally clean and obtained from extracted core material. The use of extracted core material can, in some instances, supply a "worst case" scenario. If a reservoir is oil-wet in the case of water injection, the migratory fines will generally be encapsulated and stabilized by the immobile or less mobile oil phase and fines mobilization may not be as severe as indicated by the use of clean, water-wet core. Also, the normal toluene extraction cleaning process can damage clays by removing the water of hydration causing, in general, greater susceptibility to velocity-induced damage and other apparent impairment mechanisms.

The use of preserved state core is technically preferable but has disadvantages with respect to both the cost and complexity of the tests involved. Preserved core implies the preservation of multiple phases within the core sample which can lead to complications associated with relative permeability effects. Due to the high flow rates utilized in velocity sensitivity tests, the residual saturations of oil, water, or gas can change due to an increase in capillary number within the system. Thus, while preserved samples can detect relatively severe damage due to fines mobilization, the accuracy and analysis of the data for relatively subtle changes in permeability is much more difficult.

Description of Equipment Used in Fines Migration Tests

A schematic of the experimental apparatus used in fines mobilization tests appears as Figure 1. The core sample is encased in teflon shrink tubing and placed in a 2.54 or 3.81 cm I.D., 0.635 cm heavy lead sleeve. The shrink tubing is used to ensure that no fluid slippage occurs between the sleeve and the core and prevents direct fluid contact with the lead sleeve. The ductility of the lead sleeve allows a confining overburden pressure to be transferred to the core to simulate reservoir pressure. The core, mounted within the lead sleeve, is placed inside a 7.5 cm I.D. steel core holder which is capable of simulating reservoir pressures of up to 69 MPa. This pressure is applied by filling the annular space between the lead sleeve and the core holder with light oil and then compressing the oil with a hydraulic pump to obtain the desired overburden pressure.

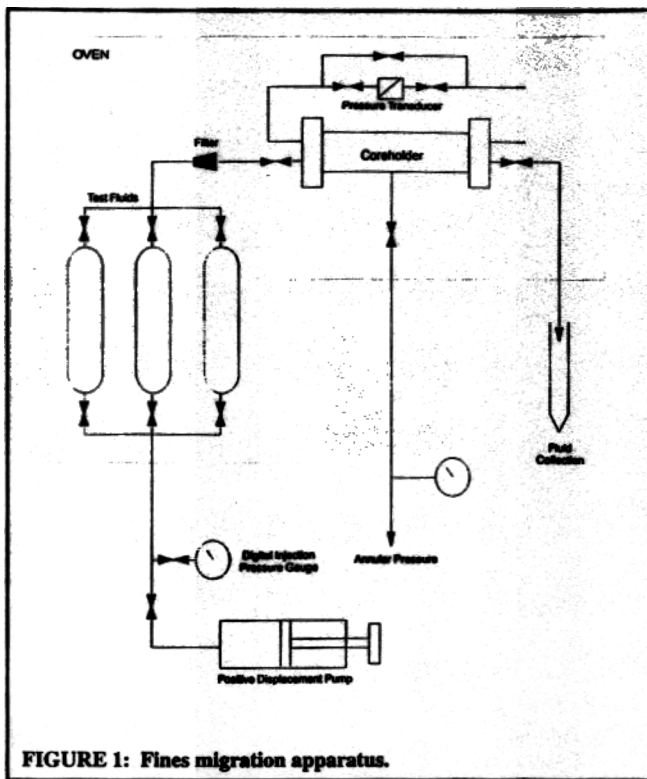


FIGURE 1: Fines migration apparatus.

The core holder ends each contain two ports. One of these ports is for fluid feed or production and the second is for pressure measurement. The portions of the core holder directly adjacent to the injection and production ends of the core are equipped with radial distribution plates to ensure evenly distributed fluid flow into and out of the core specimen.

Pressure differential is monitored using a Validyne pressure transducer. The transducer is mounted directly across the core and measures the pressure differential between the injection and production ends. The pressure transducer can have a variety of pressure ranges from 0-20 to 0-25 000 kPa depending on the expected permeability of the core material. The signal from the pressure transducer is directly connected to a strip chart recorder which provides a continuous pressure profile of the test. A digital read-out also appears on a multi-channel Validyne terminal from which the test operator takes readings as a backup. A highly accurate manometer system can also be utilized as a check on the pressure transducer measurement system.

A Ruska displacement pump is used to inject fluids into the core. The pump is capable of injecting at rates from 1 to 8200 cm³/hr at pressures up to 69 MPa with an accuracy of ± 0.01 cm³. The pump is filled with distilled water which displaces varsol. This varsol then displaces the brine to be used in the test into the core. This arrangement is used to avoid placing corrosive brine solutions directly into the pump. Effluent from the core is collected in 15 cm³ centrifuge tubes.

All injection fluids are filtered to 0.5 microns prior to use to remove any potentially plugging suspended particulates. An in-line 0.5 micron filter is also present directly before the core as a backup filtration system.

Procedure for Fines Mobilization Tests

The plug slated for the velocity sensitivity test is mounted using the equipment described. Plug or full diameter core can be utilized. The following procedure is then employed:

1. Heat to reservoir temperature, apply net overburden pressure to simulate pore pressure.
2. Evacuate core for 24 hours to remove residual gas saturation.
3. Saturate core at a low rate with filtered formation water or the non-damaging test fluid of interest.

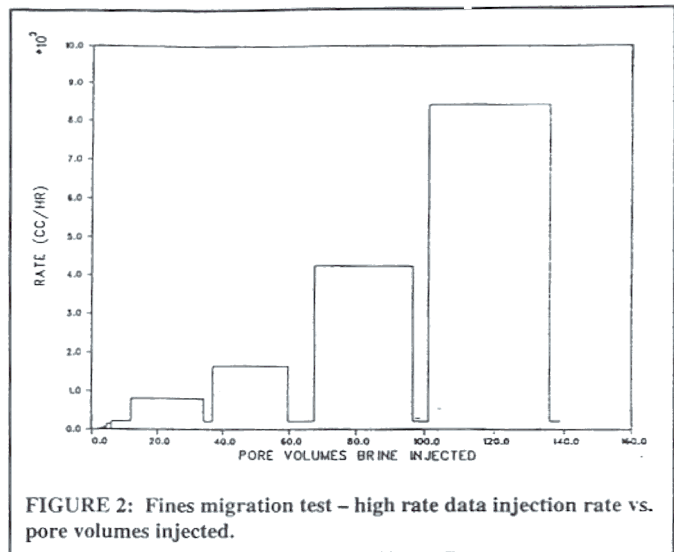


FIGURE 2: Fines migration test - high rate data injection rate vs. pore volumes injected.

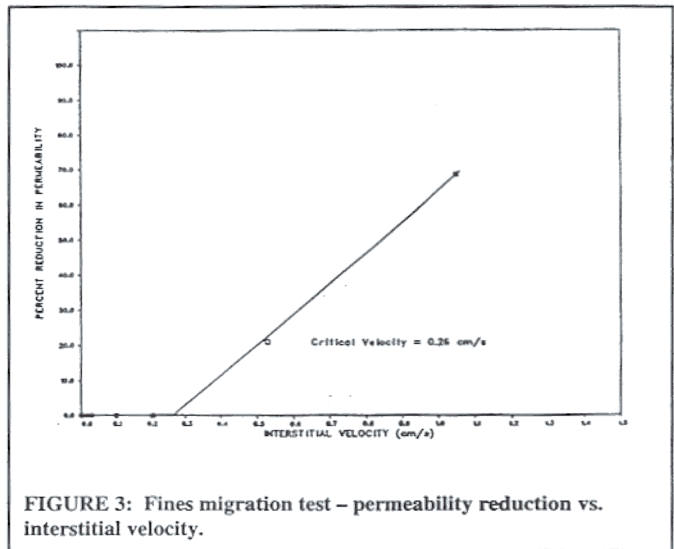


FIGURE 3: Fines migration test - permeability reduction vs. interstitial velocity.

4. Displace water through the core at a low constant rate (i.e. 20 cc/hr). Record initial absolute base permeability to brine.
5. Increase rate to 40 cc/hr, displace sufficient water to achieve steady state pressure differential. Then reduce rate to base level of 20 cc/hr and note any change in baseline permeability caused by the elevated flow rate. (Rates given are examples only and may vary according to sample permeability.)
6. Repeat step 5 at elevated rates of 60, 100, 200, 400, 1000, 2000, 4120, and 8200 cc/hr. Reduce rate back to base level to 20 cc/hr after each elevated rate displacement and measure permeability. This eliminates possible erroneous permeability measurements due to turbulence in the porous medium at high flow rates.

Figures 2 and 3 provide examples of results of a typical fines mobilization test. Figure 2 illustrates the flow sequence profile utilized in a typical fines mobilization study. The "critical" interstitial velocity for the sample in Figure 3 is about 0.26 cm/s. The damage profile represented in Figure 3 is an idealized case. Often the damage profile is not linear as illustrated and may exhibit oscillatory behavior due to the migration, entrainment and expulsion of different size distributions of fines at increasing interstitial shear rates.

Interpretation of Test Data

A problem with laboratory test data is that the critical velocity data determined is for linear flow within a porous media. Although valuable to indicate whether there is velocity-induced

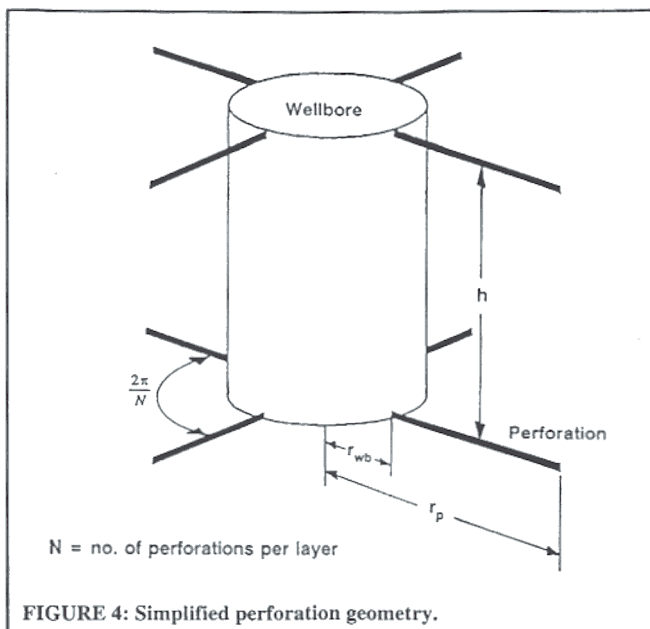


FIGURE 4: Simplified perforation geometry.

damage, it provides no direct insight into what a safe injection or production rate would be in the field.

Actual flow into or out of the reservoir is rarely simple (as in the case of an openhole completion) where a simple radial flow model can be used to evaluate the maximum sandface velocity based strictly on the hole diameter, porosity of the formation, and the net pay. More commonly, wells are cased and then perforated. This results in a very complex flow geometry governed by:

- perforation type, size and length
- perforation density (number of shots/metre)
- vertical versus horizontal permeability ratio
- porosity
- net pay
- reservoir heterogeneity
- number of open and effective perforations
- localized damage adjacent to the perforations

In order to obtain reliable estimates of the maximum velocities which will occur in the near perforation region, where potential damage will be most severe, detailed modelling of flow in this area is necessary. Formulation of such a flow model will then allow direct application of the laboratory test data back to field injection or production conditions.

Simulation Model Development

Numerous authors have conducted numerical simulations to describe the steady-state flow characteristics in the near wellbore region associated with perforated completions. The earliest studies were carried out utilizing finite difference techniques to solve the partial differential equation derived from material balance considerations of flow within a porous media. Harris⁽¹²⁾ first applied this technique in an attempt to define the productivity enhancement achieved by utilization of perforated completions as opposed to openhole completions. Hong⁽¹³⁾ also used this approach to calculate productivity ratios for various completion configurations. As computing capabilities have increased, more rigorous finite element models have been developed to define the flow patterns surrounding a perforation. More recently, Locke⁽¹⁴⁾ and Tariq⁽¹⁵⁾ have developed three-dimensional finite element models to calculate the productivity ratios associated with more complex geometrical perforation configurations, namely, helical perforation patterns. In many of these studies, nomographs have been developed to assist in the calculation of productivity ratios for various perforation configurations and to assist in ascertaining the most productive completion design.

In none of these studies, however, have velocity profiles been provided to alert engineers of the potential problems associated

with fines migration in this high-velocity flow region.

Since velocity patterns can vary significantly depending upon values of the parameters affecting flow, it is desirable to be able to simulate the flow in an efficient yet accurate manner so that flow profiles can be easily calculated for specific configurations. In view of this, the following assumptions have been incorporated in the model developed. First of all, an incompressible, single phase system is considered. Although this assumption does introduce a certain degree of error into the results, the simulation results still provide a reasonable approximation for the purpose outlined. Secondly, the near wellbore region is assumed to be characterized by a constant porosity throughout. As far as permeabilities in this region are concerned, vertical permeabilities can vary significantly from horizontal permeabilities. The model, therefore, includes specification of a horizontal permeability, which is constant in the radial plane, and a vertical permeability, which is constant in the vertical direction. A further assumption involves implementation of a simplified geometry in which multiple perforations are carried out at uniform vertical intervals in a radially symmetric manner as illustrated in Figure 4. The distance between perforation layers is easily varied to match specific perforation patterns. The number of perforations in a given layer is also adjustable to match the appropriate phase angle and shot density.

Results of previous studies reflect the need to evaluate flow in three dimensions. With the assumptions incorporated into the model, the potential equation describing flow in a steady-state system in cylindrical co-ordinates is given by the following equation:

$$\frac{\partial}{\partial r} \left(r T_r \frac{\partial P}{\partial r} \right) + \frac{1}{r} \frac{\partial}{\partial \theta} \left(T_\theta \frac{\partial P}{\partial \theta} \right) + r \frac{\partial}{\partial z} \left(T_z \frac{\partial P}{\partial z} \right) = 0$$

The pressures defined in Equation (1) are related to velocities in the manner described by Forchheimer's equation:

$$-\frac{\partial P}{\partial x} = \frac{\mu v}{k} = \beta \rho v^2$$

For low velocity flows, the second term of Equation (2) becomes negligible and the equation reduces to the well-known Darcy equation. Inclusion of the velocity-squared term, however, becomes necessary as velocities increase causing turbulence and interstitial effects in the interstices of the porous media. Since highest velocities appear at the flow-convergent region surrounding the perforation, inclusion of this turbulence term may significantly affect the magnitude of the velocities calculated. In order to incorporate Equation (2) into the solution of the potential equation, the transmissibilities defined in Equation (1) are represented by the following manipulation of Equation (2):

$$T = \frac{k}{\mu + k\beta\rho v} \quad (3)$$

Firoozabadi and Katz⁽¹⁶⁾ studied high-velocity flow through several sandstone cores and developed the following correlation for the velocity coefficient, β .

$$\beta = \frac{1.805 \times 10^{-5}}{k^{1.201}} \quad (4)$$

In order to develop an efficient, accurate model the numerical method utilized to solve the potential equation is critical. Finite difference techniques have long been employed in solving the partial differential equations in black-oil as well as compositional simulators. The drawback of finite difference approximations, however, is the introduction of truncation errors, the magnitude of which are a function of the discretization intervals selected. Of course these errors may be minimized by increasing the total number of gridblocks. In addition, solution of partial differential equations by means of finite difference techniques yields pressure results which are averaged over the gridblocks defined. For mod-

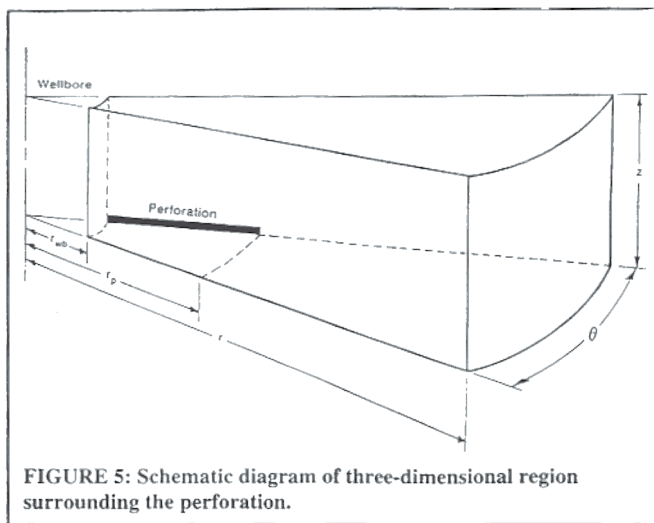


FIGURE 5: Schematic diagram of three-dimensional region surrounding the perforation.

erate gradients this is not a serious discrepancy, but again the inaccuracy associated with this approximation is a function of the grid specification.

Finite element techniques have been increasingly utilized in applications for the solution of this numerical method's formulation. Increased accuracy can be achieved by varying the sizes of the finite elements and/or the specification of higher order polynomial approximations of partial differential equations; particularly, the solution of momentum and continuity equations. This method is based upon the use of functional approximations to the solution over discrete "elements". The attractiveness of this approach lies in its ability to conform to irregular shapes or regions involving steep gradients. Due to the nature of this numerical method's formulation, increased accuracy can be achieved by varying the sizes of the finite elements and/or the specification of higher order polynomial approximations. While implementation of finite element methods hold great promise, the vast majority of reservoir simulators still employ finite difference techniques due to the substantial effort involved in the design of the finite element mesh for specific applications.

Methods of Weighted Residuals unite the finite element approach described with another technique known as Collocation. These methods, as described in Villadsen and Michelsen⁽¹⁷⁾ also employ polynomial approximations to the solution of partial differential equations with formulations such that errors at nodes chosen are zero so long as the functions are continuous and the degree of the polynomial approximations used is sufficiently high. Using families of orthogonal polynomials, these nodal points are selected as the roots of the orthogonal polynomial or collocation points. The manner in which this method is formulated facilitates adaptation of the grid which enables study for minimization of the number of grids while still maintaining accuracy. Due to the increased accuracy obtainable with this method, as compared with finite difference approximations, the orthogonal collocation technique has been applied here in solving the three-dimensional flow problem describing flow in the vicinity of the perforation. Despite the accuracy and versatility of collocation methods, the resultant matrix which must be solved is a sparse, non-uniformly-banded matrix. Hence, in order to maintain a diagonal matrix, orthogonal collocation is implemented in both the angular and vertical directions and finite difference is applied in the radial direction. In this manner, the directions in which maximum gradients are expected to occur are modelled utilizing the most accurate approximations.

Stipulation of the simplified perforation geometry dictates that the region to be simulated need cover only one-quarter of the flow area. This assumption assumes a homogeneous reservoir system with an undamaged, open perforation. This three-dimensional region is illustrated in Figure 5. Because of the symmetry of the flow patterns for the simplified geometry, each of the vertical and angular boundaries are specified by Neumann boundary conditions. Radially, the presence of the wellbore also dictates a no flow boundary. At the outermost radius, specified as 60 times the

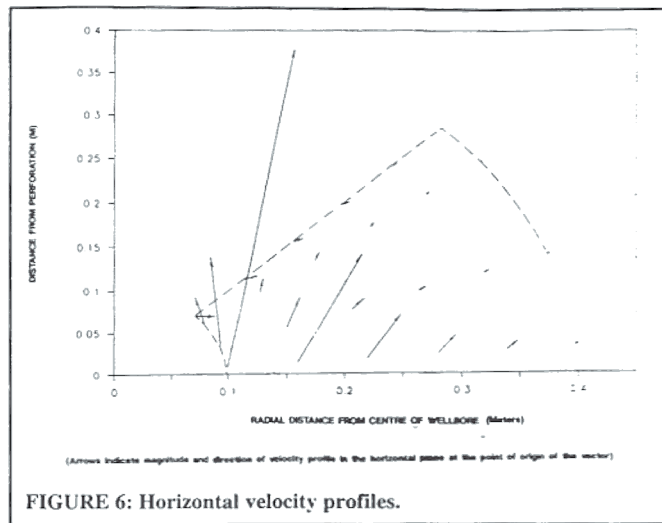


FIGURE 6: Horizontal velocity profiles.

wellbore radius, the assumption is made of perfect radial flow. As far as the actual perforation is concerned, the following equation is incorporated into the model.

$$\frac{\pi}{4} d_p^2 \frac{\partial}{\partial r} \left[T_p \frac{\partial P}{\partial r} + \frac{T_\theta}{r} \frac{\partial P}{\partial \theta} + T_z \frac{\partial P}{\partial z} \right] = 0 \quad (5)$$

Derivation of this equation is based upon the following two assumptions. Firstly, the perforation is approximated by a square cross-sectional tube whose cross-sectional area is equivalent to that of a cylinder of diameter d_p , and secondly, the perforation is represented as line source located at the intersection between the lower horizontal plane and the inner radial plane as shown in Figure 5. Saucier⁽¹⁸⁾ performed laboratory tests on pressure profiles in formation-filled and gravel-packed perforations, revealing a large range in permeabilities in perforations as a function of the nature of the porous material in them. In order to allow for this, the permeability in the perforation must be specified as an input parameter. In addition, a crushed zone at the end of the perforation can be accounted for by reduction of the radial transmissibility at that point. Angular transmissibility can also be altered to account for permeability impairment due to crushing along the perforation walls. The model has further been structured to require both a pressure at the outer boundary and a bottomhole pressure as input to the simulator. Production or injection rates, depending upon the pressure values assigned, can then be calculated from the pressure gradients calculated by the model.

Initiation of the simulation is made by use of Darcy's equation for calculation of transmissibilities. The resultant matrix is then solved using an iterative method to arrive at the nodal pressure values. From these values, velocities are calculated for each of the nodes. For high velocity flows, accommodation for turbulent flow is made by iterative correction of the transmissibility terms in accordance with Equations (3) and (4).

Simulation Results

Simulation results are obtained for a 0.20 m diameter injection well with four perforations per layer. Distance between successive layers of perforations is 0.5 m with each perforation extending out radially into the formation a distance of 0.30 m. Permeabilities in the horizontal direction have been set at 100 mD, while in the vertical direction, a permeability of 50 mD is specified. Compensation for the crushed zone at the radial end of the perforation is accounted for by a 100-fold reduction in the permeability at this point. For simplicity the walls of the perforation are assumed to be non-damaged in these examples. In most cases a zone of impaired permeability is present along the wall of the perforation (which can be taken into consideration in the input permeability specifications for the model if desired). Flow through

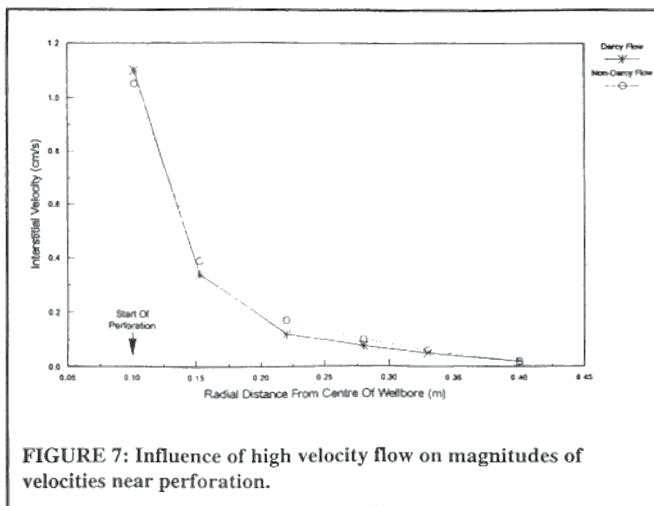


FIGURE 7: Influence of high velocity flow on magnitudes of velocities near perforation.

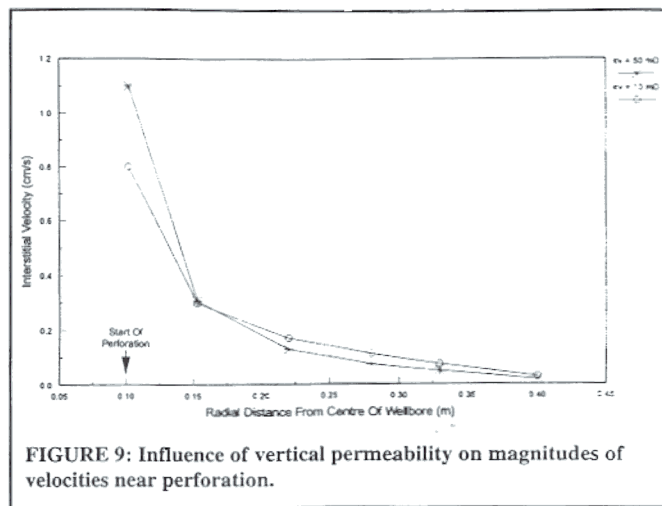


FIGURE 9: Influence of vertical permeability on magnitudes of velocities near perforation.

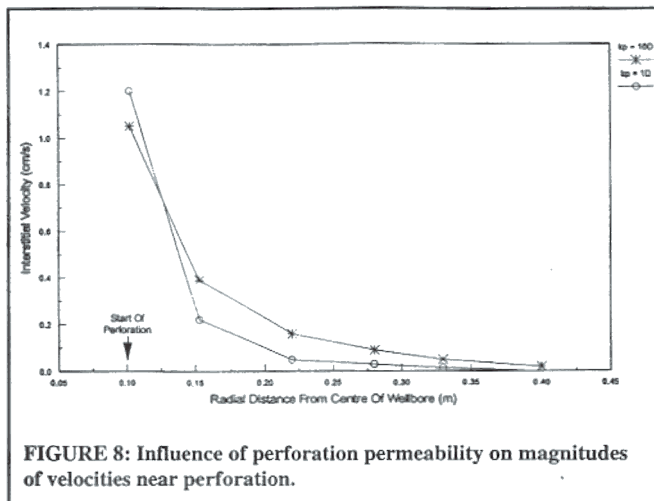


FIGURE 8: Influence of perforation permeability on magnitudes of velocities near perforation.

the perforation itself is dictated by a 10 D permeability, simulating a relatively poorly conductive packed perforation. (These are assumptions utilized strictly for this example case.)

For simulation of a water injection well, the fluid is assigned a density of 1100 kg/m³ and a viscosity of 1 mPa.s (1 cP). All pressures in the model are normalized and a simulation is carried out for an injection pressure of 1.0 and a normalized pressure specified at the outer boundary of 0.1, which translate into pressures of 20 MPa and 15.5 MPa, respectively. Solution of the resultant pressure profiles enables calculation of the injection rates based upon gradients at the outer radial boundary. Back calculation in this manner yields an injection rate of 0.630 m³/day of water into the single perforation. This is further verified by integration of the velocity gradients along the length of the perforation.

Solution of the matrix describing flow within the wellbore region is obtained by iterative correction of an initial guess of the pressure profile. The pressures calculated for each of the gridpoints then allow calculation of the velocities, which are functions of the pressure gradients. Figure 6 illustrates the velocity profiles calculated by the model assuming Darcy flow for the horizontal plane immediately adjacent to the perforation. The lengths of the arrows displayed are proportional to the magnitude of the velocities emanating from the initial points of each of the vectors in the directions shown. It should be noted that these velocity vectors do not include vertical components which also vary with distance from the perforation. Since permeabilities are largest in the horizontal direction, however, the horizontal component of the velocities with the greatest magnitudes are illustrated in this diagram. The results of the simulation reveal that the largest velocities are encountered at the perforation-wellbore interface and decrease monotonically with distance from this point. These results are intuitively expected. A further observation is the decrease in mag-

nitude of the velocity vectors along the length of the perforation. This reduction is related both to the permeability along the length of the perforation and to the presence of the crushed zone at the radial boundary of the perforation. Due to these two factors, pressures decrease rapidly along the length of the perforation which result in lower angular and vertical pressure gradients and, hence, lower velocities in each of these directions.

After calculation of the velocity profiles generated using the Darcy flow assumption, compensation for non-Darcy flow is achieved by correction of the transmissibility terms in accordance with Equation (3) followed by iterative solution of the revised matrix. While this does not significantly alter velocity profiles throughout the region, a small effect is noticeable. Comparison of velocity magnitudes for gridpoints, situated along a radial axis on the same horizontal plane as the perforation and deviating only 4.5° from the radial axis of the perforation, is provided in Figure 7. Although the injection rate into the formation is small for this particular case, allowance for non-Darcy phenomena does indicate an effect which may be much more significant for higher injection rates. As far as actual velocities are concerned, both curves indicate that velocities may be sufficient to cause fines migration near the wellbore dependent, of course, upon the actual value of the critical velocity which can be measured in laboratory fines migration tests. Of interest in the simulation results are not only the points at which fines may begin to be mobilized, but also the directions in which fines may be displaced.

Another factor demanding attention is the permeability of the perforation itself. The properties of the perforation packing material will strongly affect permeability which, in turn, will affect both the injectivity and the nature of the velocity profiles. In order to investigate this, a separate run is carried out for the same conditions, but with a very low permeability in the perforation of only 1 D (this simulates a badly infilled gravel packed perforation). Simulation results indicate that this reduction causes the overall injection rate to decrease to 0.376 m³/day. The comparison of velocity magnitudes (along the same radial axis described in Figure 6) for this case, in contrast to those for the base case, are shown in Figure 8. As anticipated, the reduction in perforation permeability causes greater flow velocity out of the perforation at the perforation-wellbore interface and decreased flow velocity further along its length.

Reservoir geology and perforation patterns will also affect flow – both in terms of injectivity and velocity profiles surrounding the perforation. The magnitude of the effects caused by variations in either reservoir geology or the perforation pattern, however, are difficult to quantify. For example, another run carried out for the case of a 10 mD vertical permeability ($k_v/k_r = 10$ as compared with $k_v/k_r = 2$ for the base case) indicates a total injection rate of 0.596 m³/day, a reduction of only 5%. As far as velocities are concerned, a comparison of velocity magnitudes is presented in Figure 9. In comparison with the magnitude of the velocities observed in the base case, the reduction in vertical permeability

results in lower velocities near the wellbore, but higher velocities radially outward. While this is an expected consequence of a vertical flow restriction which results in higher pressures (i.e. lower pressure gradients) near the wellbore and, consequently, higher velocities at greater radial distances, the magnitude of the differences is difficult, if not impossible, to ascertain without the use of a simulation.

Conclusions

Fines migration is a source of potentially severe permeability impairment. Laboratory tests have been developed and equipment has been constructed to determine critical velocities at which fines begin to mobilize. Laboratory procedures facilitate the calculation of these critical velocities which represent linear flows within porous media. In order to apply this information to an actual reservoir, a three-dimensional simulator has been developed to calculate the velocity profiles surrounding a perforation. Although not discussed in this paper, development of this model enables modification of reservoir geological properties (i.e. permeabilities) and perforation patterns, including the number of perforations per layer, the permeability of the perforation, and the length and diameter of the perforation. In addition, allowance is made for non-Darcy flow, a phenomenon which may become significant in the high velocity flow region surrounding a perforation. Due to the complex nature of three-dimensional flow, this type of a simulation is necessary to quantify velocity profiles and thus apply the results of laboratory experimentation.

Acknowledgements

The assistance and technical expertise of staff at Hycal Energy Research Laboratories Ltd. are greatly appreciated.

NOMENCLATURE

d_p	= Diameter of Perforation (m)
k	= Permeability (D)
r	= Radial Distance (m)
v	= Velocity (m/s)
z	= Vertical Distance (m)
P	= Pressure (kPa)
T	= Transmissibility (D/Pa.s)

Greek Symbols

β	= Non-Darcy Coefficient (m/D)
μ	= Fluid Viscosity (Pa.s)
θ	= Angular Distance (rad)

Subscripts

r	= Radial
θ	= Angular
z	= Vertical
a	= areal

REFERENCES

- MUECKE, T.W., Formation Fines and Factors Controlling Their Movement in Porous Media; *Journal of Petroleum Technology*, February, 1979, pp. 144-50.
- GRAY, D.H. and REX, R.W., Formation Damage in Sandstone Caused by Clay Dispersion and Migration; *Clay and Clay Minerals*, p. 26, 1966.
- MORGAN, J.T. and GORDON, D.T., Influence of Pore Geometry on Water-Oil Relative Permeabilities; *Journal of Petroleum Technology*, October, 1970, pp. 1199-1208.
- PORTER, K.E., An Overview of Formation Damage; *Journal of Petroleum Technology*, Vol. 41, No. 8, August, 1989.
- SELBY, R.J., and FAROUQ-ALI, S.M., Mechanics of Sand Production And The Flow of Fines in Porous Media; *Journal of Canadian Petroleum Technology*, Vol. 27, No. 3, May, 1988, pp. 55-63.
- KWAN, M.Y., CULLEN, M.P., JAMIESON, P.R. and FORTIER,

R.A., A Laboratory Study of Permeability Damage to Cold Lake Tar Sands Cores; *Journal of Canadian Petroleum Technology*, Vol. 28, No. 1, February, 1989., pp. 56-62.

- PRISHOLM, S., NIELSON, B.L. and HASLUND, O., Fines Migration, Blocking, and Clay Swelling of Potential Geothermal Sandstone Reservoirs: Denmark, Society of Petroleum Engineers Form Evaluation, June 1987.
- GABRIEL, G.A. and INAMDAR, G.R., An Experimental Investigation of Fines Migration in Porous Media; Society of Petroleum Engineers Paper 12168, presented at the 1983 Society of Petroleum Engineers Annual Technical Conference and Exhibition, San Francisco, CA, October 5-8, 1983.
- BORCHARDT, J.K., ROLL, D.L. and RAYNE, L.M., Use of a Mineral Fines Stabilizer in Well Completions; Society of Petroleum Engineers Paper 12757, presented at the 1984 Society of Petroleum Engineers California Regional Meeting, Long Beach, CA, April 11-13, 1984.
- SENGUPTA, S.K. et al., Effect of Flow Rate and Rheology on Shear Strength of Migrating Formation Fines Due to Flow of Pseudoplastic Fluids; Society of Petroleum Engineers Paper 10669, presented at the 1982 Society of Petroleum Engineers Formation Damage Control Symposium, Lafayette, Los Angeles, CA, March 24-25, 1982.
- GRUESBECK, C. and COLLINS, R.E., Entrainment and Deposition of Fine Particles in Porous Media; Society of Petroleum Engineers Journal, December 1982, pp. 846-56.
- HARRIS, M.H., The Effect of Perforating on Well Productivity; *Journal of Petroleum Technology*, April 1966, pp. 518-28; Trans. AIME, 237.
- HONG, K.C., Productivity of Perforated Completions in Formations With or Without Damage; *Journal of Petroleum Technology*, August 1975, pp. 1027-38; Trans., AIME, 259.
- LOCKE, S., An Advanced Method for Predicting the Productivity Ratio of a Perforated Well; *Journal of Petroleum Technology*, December 1981, pp. 1381-88.
- TARIQ, S.M., Evaluation of Flow Characteristics of Perforations Including Nonlinear Effects With the Finite-Element Method; Society of Petroleum Engineers, May 1987, pp. 104-112.
- FIROOZABADI, A. and KATZ, D.L., An Analysis of High-velocity Gas Flow Through Porous Media; *Journal of Petroleum Technology*, February 1979, pp. 211-16.
- VILLADSEN, J. and MICHELSEN, M.L., Solution of Differential Equation Models by Polynomial Approximation; Prentice-Hall Inc., New Jersey, 1978.
- SAUCIER, R.J., Considerations in Gravel Pack Design; Society of Petroleum Engineers, February, 1974, pp. 205-212. ‡

Authors' Biographies

John Eng is currently working on his Ph.D. at Brigham Young University in Utah. John was employed by Hycal Energy Research Laboratories Ltd. as a Senior Research Engineer working in the area of numerical modelling and multi-phase flow in porous media. John received B.Sc. and M.Sc. degrees from the University of Calgary in Chemical Engineering and is a member of APEGGA.



Brant Bennion is currently President of Hycal Energy Research Laboratories Ltd. of Calgary, Alberta. He is involved in research in multi-phase flow in porous media, formation damage studies, miscible and thermal E.O.R. Brant received a B.Sc. from the University of Calgary in 1984 and is a member of APEGGA and a Board member of the Calgary section of The Petroleum Society of CIM.



Jeff Strong is currently a Senior Research Engineer at Hycal Energy Research Laboratories Ltd. Jeff's interests include fluid phase behavior and formation damage. Jeff received a B.Sc. degree from the University of Calgary and is a member of APEGGA and The Petroleum Society of CIM.